

# Fabrication and enhanced optical absorption of submicrometer pits array on 6H-SiC via two-beam interference of femtosecond laser

Yi Zhang (张艺), Xin Jia (贾鑫), Pingxin Xiong (熊平新), and Tianqing Jia (贾天卿)\*

State Key Laboratory of Precision Spectroscopy, Department of Physics, East China Normal University, Shanghai 200062, China

\*E-mail: tqjia@phy.ecnu.edu.cn

Received June 24, 2010

We report the fabrication of submicrometer pits array (SP-array) on 6H-SiC surface by the interference of two femtosecond laser beams. Formation mechanisms and optical absorption of SP-array are studied. The relative reflectivity and transmissivity of white light decrease to 10% of the values of SiC crystal, and the optical absorption is enhanced to 97%. The relative reflectivity and transmissivity of incident angles within the range of 20°–60° are kept below 25%. The enhancement mechanism of optical absorption of the SP-array is also discussed.

OCIS codes: 320.7130, 220.4241, 110.4235.

doi: 10.3788/COL20100812.1203.

Optical absorption is one of the key factors that determine the usage efficiency of solar energy<sup>[1]</sup>. Texturing the front surface of a semiconductor is an efficient method to improve optical absorption<sup>[2,3]</sup>. Optical absorption enhancement of silicon, which is very important for silicon-based solar cells, has been investigated intensively. Several kinds of microstructures and nanostructures, such as microspikes<sup>[4]</sup>, nanowires, and nanocones array<sup>[5,6]</sup>, have been reported recently.

Femtosecond laser-induced microstructures in dielectrics and semiconductors have been studied intensively<sup>[7–12]</sup>. Optical waveguide, micro-mirrors, and other functional micro-devices have been reported. Recently, periodic nanoripples in semiconductors and dielectrics were fabricated by femtosecond laser<sup>[13–16]</sup>, and the optical absorption was greatly enhanced on the structured surface<sup>[2]</sup>.

SiC is a wide band-gap semiconductor that has attracted increasing attention due to its outstanding electrical, chemical, mechanical, and thermal properties<sup>[17]</sup>. In this letter, we report a new microstructure on 6H-SiC, the so-called submicrometer pits array (SP-array), which is induced by the interference of two femtosecond laser beams. Compared with the SiC crystal surface, the relative reflectivity and transmissivity in the structured surface reduce dramatically to 11.8% and 10.1%, respectively. The formation mechanisms of the SP-array and the optical absorption enhancement are also studied.

A linearly polarized laser at 800-nm wavelength with a pulse duration of 50 fs was delivered from a commercial Ti:sapphire regenerative amplifier operated at repetition rates of 1–1000 Hz (Legend Elite, Coherent). A half-wave plate and a Glan polarizer were used to adjust the intensity and polarization of the laser pulses. The laser beam was split into two beams with the same intensity and polarization by a beam splitter, and the two beams were then overlapped simultaneously on the SiC crystal surface. The cross angle of the two laser beams was 13.9°. Zero temporal point was determined by the signal of sum frequency via a  $\beta$ -barium borate (BBO) crystal.

In the experiment, a He-Ne laser beam was irradiated on the ablation area to investigate the change of diffraction light.

A square 6H-SiC crystal 10×10×1 (mm) in size was mounted on an XYZ translation stage controlled by a computer. By translating the sample, we can ablate the surface spot by spot and obtain a large area with SP-array. After laser irradiation, the sample was dipped in ethanol and cleaned with an ultrasonic cleaner to remove the dust and plume deposited on the sample surface.

Figure 1 shows the SP-array on 6H-SiC. The one-dimensional (1D) periodic grating structure is determined by the two-beam interference. Angle  $2\theta$  between the two beams is 13.9°, and the period is calculated to be 3.31  $\mu\text{m}$  ( $\Lambda = \lambda/2\sin\theta$ ), which agrees well with the experimental value of 3.3  $\mu\text{m}$  (see Fig. 1). Quasi-periodic submicrometer pits aligned along the grating direction formed the two-dimensional (2D) SP-array. The sample was cut to observe the cross section. Hole diameter was 700–900 nm and the depth was 500–700 nm.

To study the formation mechanism of SP-array, the surface morphologies for different irradiation times were observed. Figure 2 shows a series of scanning electron microscope (SEM) images of the structured SiC surface in the central part of the ablation crater. Periodic ripples were formed on the stripes with peak intensity after 1-s irradiation time. The ripple period is close to the laser wavelength ( $\sim 800$  nm), and the orientation is perpendicular to the laser polarization. The ripples were induced by the interference of the incident laser and the surface scattering light<sup>[18,19]</sup>. The energy of the following pulses was mostly deposited in the ripple grooves when the radiation time was increased. This mechanism was a result of inhomogeneous absorption. Therefore, the grooves became deeper and wider, as shown in the pictures of 3 and 5 s. The size of the grooves increased with longer irradiation time. The SP-array was formed after 10-s irradiation. In the formation process, two-beam interference played an important role in the periodic intensity distribution that limited the ripple length. Only

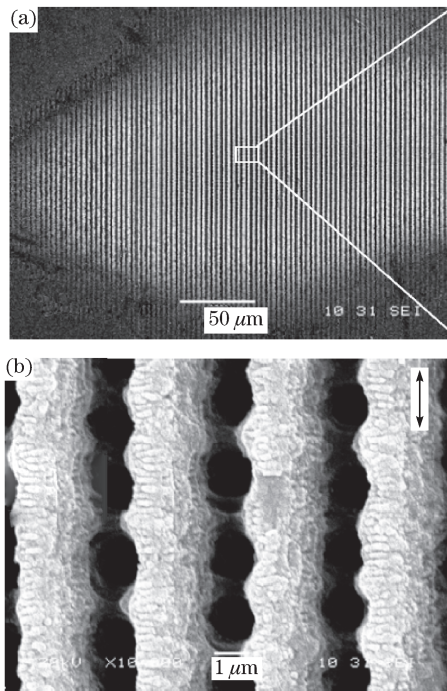


Fig. 1. (a) SEM image of the SP-array induced by the two-beam interference. The laser fluence of single beam is  $1.0 \text{ J/cm}^2$ , repetition rate is 10 Hz, and irradiation time is 10 s. (b) Enlarged view of square area of (a). The arrow bar in (b) represents the laser polarization.

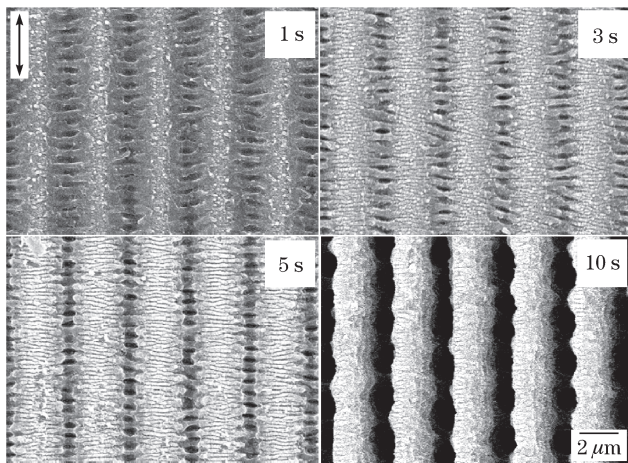


Fig. 2. SP-array evolution with the laser irradiation time. The laser fluence of single beam is  $1.0 \text{ J/cm}^2$  and repetition rate is 10 Hz.

the depth and width of ripple grooves increase with the irradiation time.

The SP-array can be formed only when the laser intensity is high enough. If the laser fluence of a single laser beam is less than  $0.5 \text{ J/cm}^2$ , there is no SP-array in the ablation area.

Diffraction and diffusion of the He-Ne laser change greatly with increasing laser irradiation time. These changes can be described in four processes. (a) When the irradiation time is less than 1 s, the zero-order diffraction peak is much greater than the higher-order ones because the grating has not formed. (b) Regular grating gradu-

ally forms beyond 1-s irradiation time. The higher-order diffraction peaks become stronger, whereas the zero-order diffraction peaks weaken. The diffraction peaks become the strongest at 5-s irradiation time. (c) Increased diffused light is observed at 5–7-s irradiation time. All the zero-order and the higher-order diffraction peaks decrease with the formation of SP-array. (d) Intensities of diffraction and diffusion light are reduced dramatically at over 7-s irradiation time. Diffraction peaks become nearly invisible as the SP-array is formed. The reflected and the transmitted processes are similar to each other. These results indicate that SP-array may reduce reflectivity and transmissivity, which means optical absorption enhancement of the He-Ne laser.

Reflection and transmission spectra were measured before and after laser irradiation to study the optical absorption enhancement of white light of the structured SiC crystal. The white light source with wavelengths of 450–750 nm was produced by focusing 800-nm femtosecond laser pulses into a water cell. The white light was then focused on the planar surface and the central part of the ablation craters through a  $5\times$  Nikon objective lens at an incident angle of  $40^\circ$ . The reflected and transmitted lights were collected by a lens with 50-mm focal length and 25-mm diameter. The sketch of the reflection-collection setup is shown in the inset of Fig. 3(a). The lens was set at the position of 36 mm in front of the sample. Hence, the collected angle  $2\alpha$  was about  $70^\circ$ . To eliminate the influence of diffusion light, the spectra for various divergence angles  $\beta$  were measured. Figures 3(a) and (b) show the diffusion spectra in the horizontal ( $x$ - $y$  plane) and vertical ( $x$ - $z$  plane) directions, respectively. The light in the range of  $0^\circ$ – $35^\circ$  was collected while that beyond  $35^\circ$  was excluded. In the horizontal direction, the light decreased to nearly zero when the angle  $\beta$  was beyond  $35^\circ$  (see Fig. 3(a)). Similarly, the light weakened rapidly in the vertical direction. The ratio between the uncollected and collected lights was calculated by integrating the spectra in the range of 450–750 nm. A rough estimation of no more than 25% was achieved. The case of transmission spectra was similar to the reflection case.

Figures 3(c) and (d) show the relative reflection and transmission spectra expressed as the ratio between the structured and planar surfaces under various irradiation time. Here, 25% diffusion light was taken into account. The total relative reflectivities were reduced to 32.2%, 22.9%, and 17.1% of the unstructured area for the irradiation time of 1, 3, and 5 s, respectively. The relative transmissivity values were 63.7%, 38.3%, and 15.7%, respectively. Relative reflectivity and transmissivity of the SP-array (10 s) were dramatically decreased to 11.8% and 10.1%, respectively. Results were considered as the saturation values. Obvious decrease in reflectivity and transmissivity was not observed with the further increase of irradiation time.

We have studied the formation of the SP-array with different laser fluences. Results showed that the pits array emerged rapidly for higher laser fluences, and the absorption increased accordingly. Therefore, for a given exposure time, absorption is higher for higher laser fluences.

By ablating the sample spot by spot, we obtained a

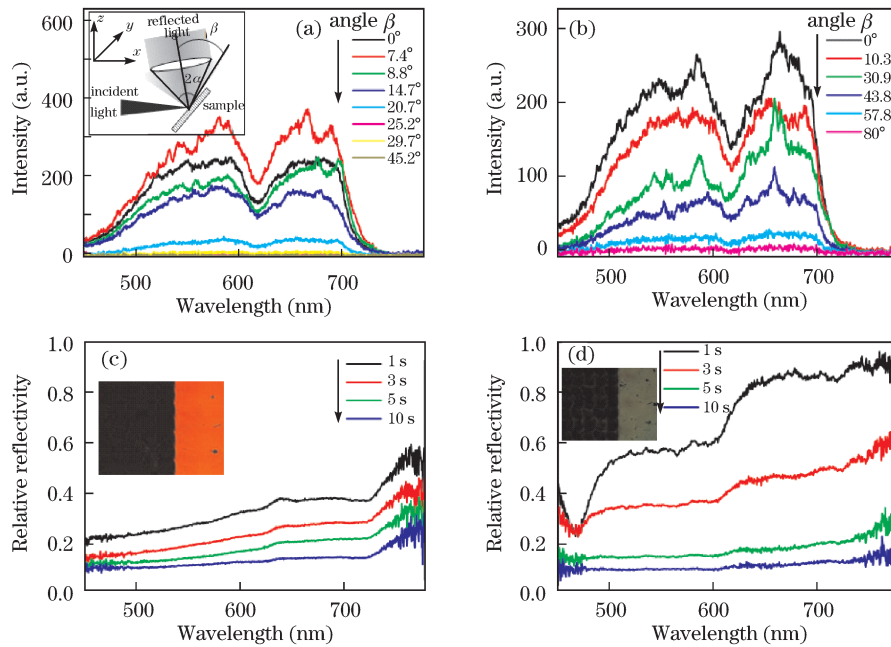


Fig. 3. Diffused spectra as a function of the divergence angles  $\beta$  in (a) horizontal and (b) vertical directions, respectively. The inset in (a) is the sketch of collection setup. (c) Relative reflection and (d) transmission spectra for different irradiation times.

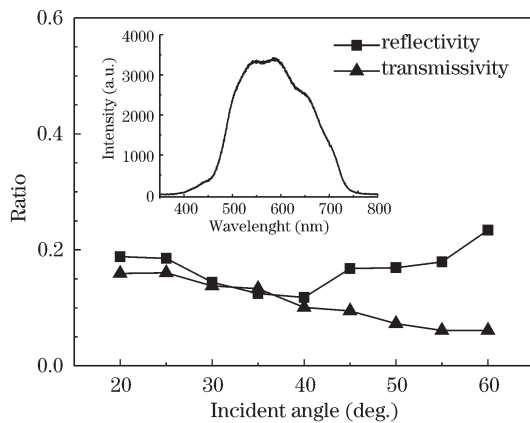


Fig. 4. Dependences of the relative reflectivity and transmissivity on the incident angles. The inset is the spectrum of white light.

large area of SP-array, with a size of  $1.5 \times 3$  (mm). The insets in Figs. 3(c) and (d) show the microscope photographs (Nikon-80i) of a part of the large-area with SP-array on reflected (inset of Fig. 3(c)) and transmitted (inset of Fig. 3(d)) illumination modes, respectively. The left dark side of the picture displays the SP-array structure, which is much darker than the unstructured area on the right side.

We measured the relative reflectivity and transmissivity of the large-area with the SP-array structure as a function of the incident angle of white light. The relative reflectivity was less than 25% in the range of  $20^\circ$ – $60^\circ$ . Minimum value was at the angle of  $40^\circ$ . The relative transmissivity decreased smoothly with the incident angle. Optical absorption was greatly enhanced in the incident angle of  $20^\circ$ – $60^\circ$ .

We proposed that the relative reflectivity and transmissivity were greatly decreased for the enhanced absorption of the structured surface. The SP-array struc-

ture increased the surface area compared with the planar surface, which resulted in absorption enhancement. In addition, the incident light can be trapped in the submicrometer pits by total internal reflection, which results in repeated absorption. Energy-dispersive X-ray (EDX) analysis on the SiC crystal indicates that the SiC crystal contains an impurity of about 0.59% Sn, which may be the main absorber.

In conclusion, the SP-array is obtained on 6H-SiC crystal by the interference of two femtosecond laser beams. The evolution of the surface morphology with laser irradiation time indicates that the SP-array evolves from long-periodic surface ripples. The reflection and transmission spectra in the range of 400–750 nm are measured before and after laser irradiation. The relative reflectivity and transmissivity dramatically decrease to 11.8% and 10.1% of the unstructured sample values, respectively. The relative reflectivity and transmissivity for the incident angle in the range of  $20^\circ$ – $60^\circ$  are kept less than 25%. The absorption is higher than 97%, which is nearly equal to the values obtained on SiC nanostructured surface<sup>[6]</sup>.

This work was supported by the Shanghai Leading Academic Discipline Project (No. B408), the National “973” Project of China (Nos. 2006CB806006, 2006CB921105, and 2010CB923203), the National Natural Science Foundation of China (Nos. 10874044 and 10904038), the Ministry of Education of China (No. 30809), the Shanghai Municipal Science and Technology Commission (Nos. 09142200500, 09JC1404700, 08JC1408400, 09ZR1409300, and 08PJ1404800), and the Twilight Project sponsored by the Shanghai Education Committee (No. 07SG25).

## References

1. J. H. Werner, S. Kolodinski, and H. J. Queisser, Phys. Rev. Lett. **72**, 3851 (1994).

2. Q. Z. Zhao, F. Ciobanu, S. Malzer, and L. J. Wang, *Appl. Phys. Lett.* **91**, 121107 (2007).
3. P. Campbell, *J. Opt. Soc. Am. B* **10**, 2410 (1993).
4. C. Wu, C. H. Crouch, L. Zhao, J. E. Carey, R. Younkin, J. A. Levinson, E. Mazur, R. M. Farrell, P. Gothoskar, and A. Karger, *Appl. Phys. Lett.* **78**, 1850 (2001).
5. L. Hu and G. Chen, *Nano Lett.* **7**, 3249 (2007).
6. J. Zhu, Z. Yu, G. F. Burkhard, C.-M. Hsu, S. T. Connor, Y. Xu, Q. Wang, M. McGehee, S. Fan, and Y. Cui, *Nano Lett.* **9**, 279 (2009).
7. S. Matsuo, S. Kiyama, Y. Shichijo, T. Tomita, S. Hashimoto, Y. Hosokawa, and H. Masuhara, *Appl. Phys. Lett.* **93**, 051107 (2008).
8. F. He, Y. Cheng, L. Qiao, C. Wang, Z. Xu, K. Sugioka, K. Midorikawa, and J. Wu, *Appl. Phys. Lett.* **96**, 041108 (2010).
9. K. Sugioka, Y. Cheng, K. Midorikawa, F. Takase, and H. Takai, *Opt. Lett.* **31**, 208 (2006).
10. T. Jia, M. Baba, M. Suzuki, R. A. Ganeev, H. Kuroda, J. Qiu, X. Wang, R. Li, and Z. Xu, *Opt. Express* **16**, 1874 (2008).
11. Y. Dong, X. Yu, Y. Sun, Y. Li, X. Hou, and X. Zhang, *Chin. Opt. Lett.* **5**, 191 (2007).
12. Y. Wu, C.-Y. Wang, W. Jia, X. Ni, M. Hu, and L. Chai, *Chin. Opt. Lett.* **6**, 51 (2008).
13. Y. Shimotsuma, P. G. Kazansky, J. Qiu, and K. Hirao, *Phys. Rev. Lett.* **91**, 247405 (2003).
14. N. Yasumaru, K. Miyazaki, and J. Kiuchi, *Appl. Phys. A* **76**, 983 (2003).
15. G. Miyaji and K. Miyazaki, *Opt. Express* **16**, 16265 (2008).
16. F. Costache, M. Henyk, and J. Reif, *Appl. Surf. Sci.* **186**, 352 (2002).
17. N. G. Wright, A. B. Horsfall, and K. Vassilevski, *Mater. Today* **11**, 16 (2008).
18. J. E. Sipe, J. F. Young, J. S. Preston, and H. M. van Driel, *Phys. Rev. B* **27**, 1141 (1983).
19. J. Young, J. S. Preston, H. M. van Driel, and J. E. Sipe, *Phys. Rev. B* **27**, 1155 (1983).